Electronic Supplementary Material (ESI) for ChemComm.

Fabrication of flexible electrode with trace Rh based on Polypyrrole for hydrogen evolution reaction

Tiantian Li, You Li, Wenhao Li, Shijie Jia, Xijie Chen, Xin Zhang* and Fengchun Yang*

Key Laboratory of Synthetic and Natural Functional Molecule Chemistry (Ministry of Education), College of Chemistry and Material Science, National Demonstration Center for Experimental Chemistry Education, Northwest University, Xi'an, 710127, China.

*E-mail：fyang@nwu.edu.cn (F. Yang), zhangxin@nwu.edu.cn (X. Zhang)

1. Experimental Section

1.1 Chemicals and Reagents.

ITO, Rhodium trichloride monohydrate ($RhCl_3 \cdot H_2O$, 99%)，concentrated sulfuric acid, pyrrole (Py, 0.968-0.971 g/mL, ⩾98%), The deionized water for solution preparation was from a Millipore Autopure system (18.20 MΩ, Millipore Ltd., USA)

1.2 Preparation of PPy/Rh on ITO

At first, the appropriate amount of $RhCl_3$ H_2O is dissolved in deionized water and stirred to obtain a 0.01 M $RhCl_3$ H_2O solution. And then H_2SO_4 and Py are added to obtain a mixed solution with 0.01 M H_2SO_4 and 0.02 M Py.

ITO are washed by H_2SO_4, deionized water and acetone for 20 min, separately. And then, ITO are cut into 1×2 cm size, and electrode clamp is used as the working electrode. Electrodeposition process is carried out in a three-electrode system with Ag/AgCl electrode as the reference electrode, Pt as the counter electrode, and the electrolyte is above preparation. PPy/Rh films are obtained by alternating deposition of 0.8 V and -0.4 V respectively with a multi-potential steps. This work shows five deposition times (55 s, 150s, 240s, 350s and 500 s). The obtained films are denoted as PPy/Rh_{55s}, PPy/Rh_{150s} PPy/Rh_{240s} PPy/Rh_{350s} and PPy/Rh_{500s}, respectively.

1.3 Characterization

XRD (Rigaku D/Max-2400, USA) with high-intensity Cu Kα radiation (λ = 1.5406 Å) is used to investigate the crystallographic structure. The Raman spectra were recorded for different parts of the film at random locations using Ar Ion Laser Source with wavelength of 633 nm, which showed no significant difference. XPS (ESCALAB250xi, USA) is used to study the chemical valence of the catalysts. A CHI 760E electro chemical workstation (CH Instruments) was used as the workstation throughout the entire electrochemical testing.

1.4 Electrochemical measurements

All the electrochemical measurements were carried out in a typical three-electrode system with all electrode connected to a CHI760E Electrochemical Workstation (CHII instruments, Shanghai Chenhua Instrument Corp. China). All the potential is converted to standard hydrogen electrode. The formula of convert the potential to RHE is: E_{RHE} =

E +0.1981+0.059*PH, where E is the potential shown in the electrochemistry workstation, and 0.1981 is the potential relative to standard hydrogen electrode, PH is the PH of electrolyte

1.5 water splitting

As for PPy/Rh_{350s}//RuO_2, the two-electrode system is composed of the cathode of Rh/PPy and RuO_2 work as anode, which are connected to the electrochemical workstation with the electrolyte of 0.5 M H_2SO_4. And the Pt/C//RuO_2 is replaced the Rh/PPy to Pt/C.

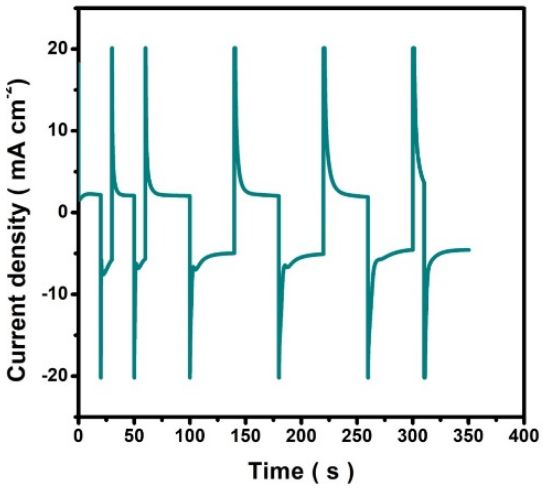

Fig. S1. Deposition curve of Rh/PPy$_{350}$ with Multi-potential steps.

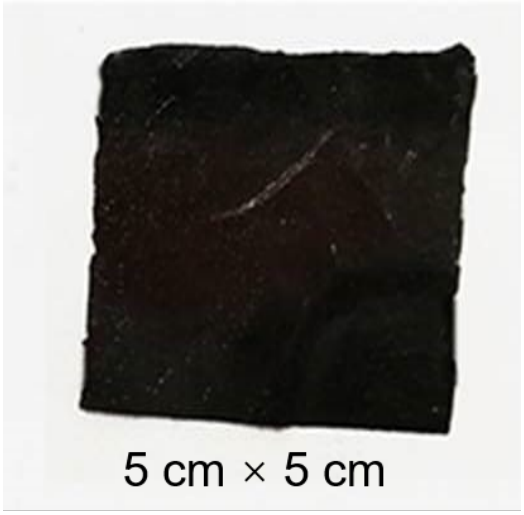

Fig. S2. The photograph of Rh/PPy$_{350}$ film peeled off from ITO after soaking in hot water several minutes with the size of 5 cm× 5 cm.

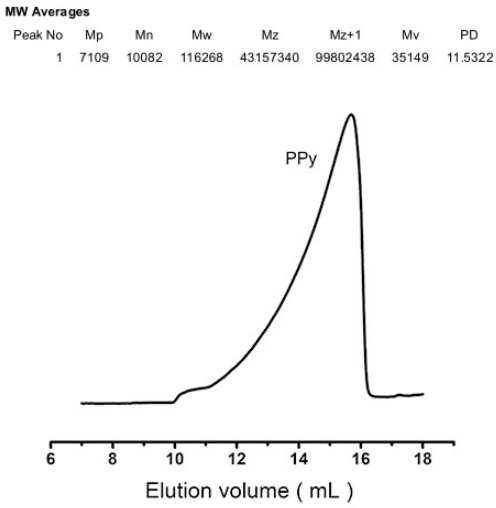

Fig. S3. GPC of PPy film.

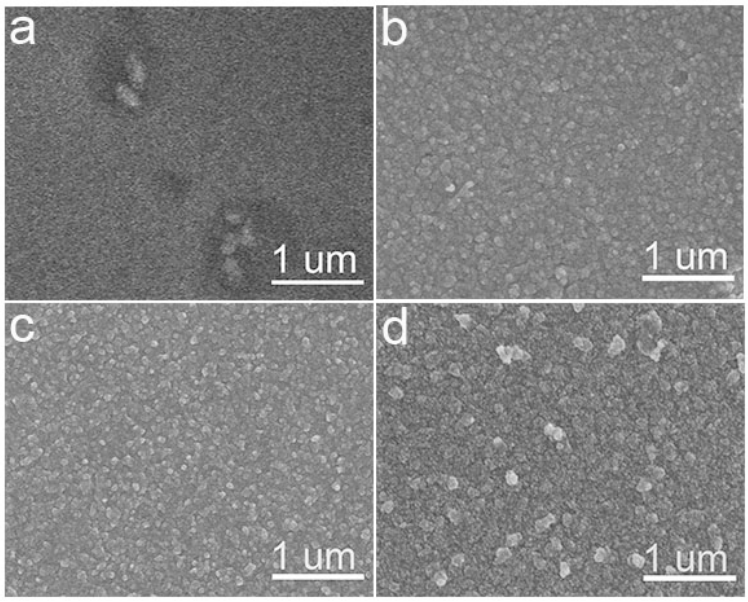

Fig. S4. SEM of Rh/PPy with the deposition time of a) 55 s; b) 150 s; c) 240 s and d) 500 s.

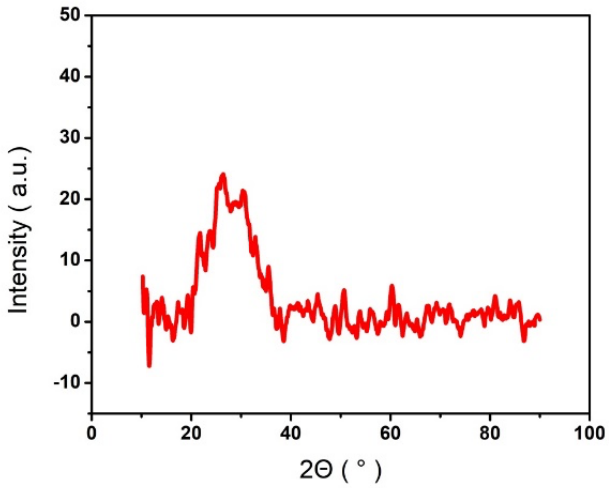

Fig. S5. The XRD of PPy.

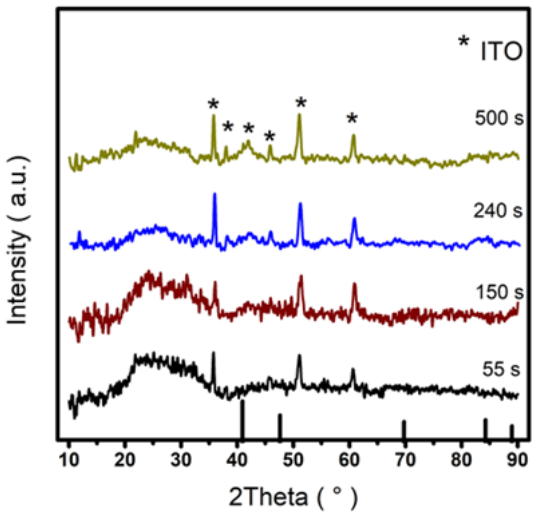

Fig. S6. The XRD of Rh/PPy with the different deposition time.

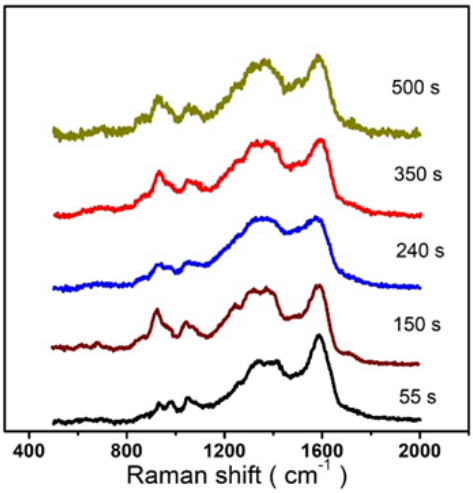

Fig. S7. The Raman specture of Rh/PPy with the different deposition time.

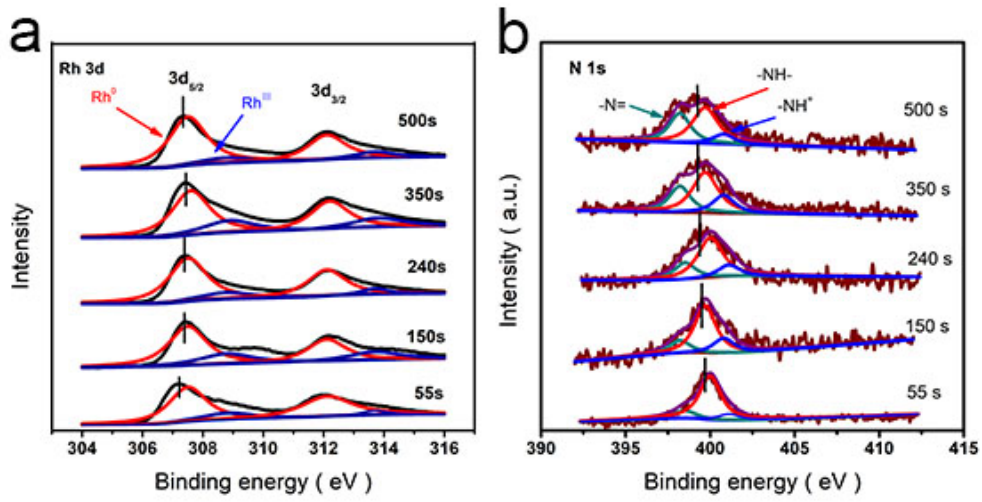

Fig. S8. a) The Rh 3d core-level spectrum and b) The N 1s core-level spectrum of Rh/PPy with the different deposition time.

Table S1. The Raman shift of C=C and C-N.

Material	C=C(cm^{-1})	C-N(cm^{-1})
PPy	1579	1368
Rh/PPy_{55s}	1588	1335
Rh/PPy_{150s}	1590	1333
Rh/PPy_{240s}	1594	1328
Rh/PPy_{350s}	1596	1318
Rh/PPy_{500s}	1580	1361

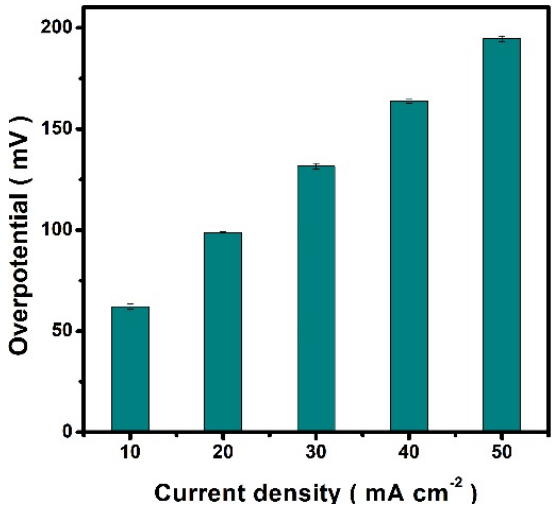

Fig. S9. The mean deviation error bars for HER, and each experiment is performed five times.

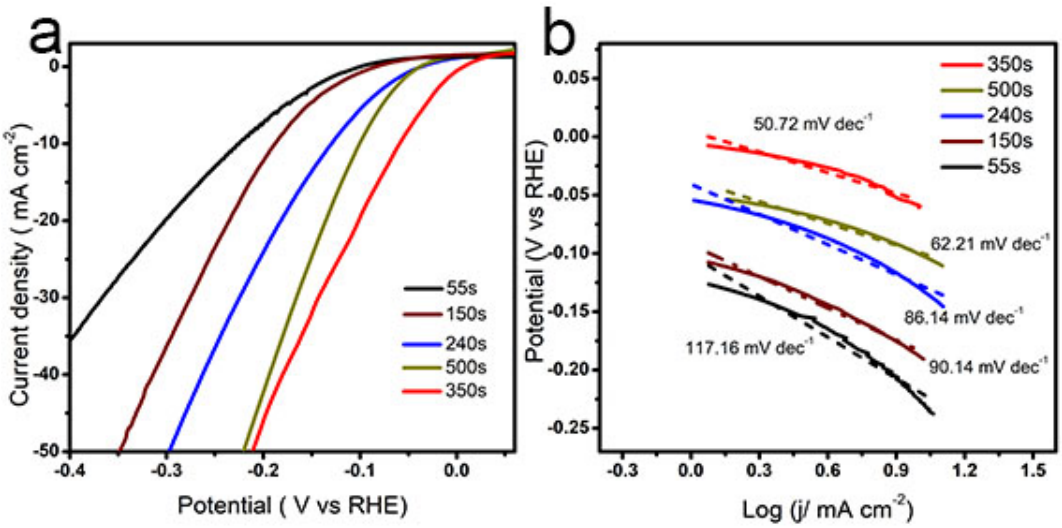

Fig. S10. a) HER polarization curves; b) Tafel plots of Rh/PPy with the different deposition time.

Table S2. The loading of Rh in Rh/PPy films with different deposition time

	Rh/PPy_{55s}	Rh/PPy_{150s}	Rh/PPy_{240s}	Rh/PPy_{350s}	Rh/PPy_{500s}
Rh loading ($mg\ cm^{-2}$)	/	0.00192	0.01024	0.01576	0.02424

Table S3. Comparison of the HER electrocatalytic performance between as-prepared Rh/PPy films and recent reported noble-metal-based electrocatalysts.

catalyst	$\eta_{10mA\ cm-2}$ (mV)	Tafel slope (mV dec^{-1})	Loading (mg cm^{-2})	References
Rh/C	41.6	113	-	S1
Rh/XC-72	43	99	0.150	S2
Rh/F-graphene	46	30	0.113	S3
Rh/Graphene	66	39	0.113	
Rh-Au/Si NW	62	24	0.260	S4
Rh/Si NW	75	24	-	S5
$Rh_3Pb_2S_2$	87	46	0.141	S6
Rh/CeO_2	42	34	0.086	S7
Rh_2S_3	117	44	-	S8
$Rh-MoS_2$	47	24	0.309	S9
Rh/Ni@NCNTs	45	21	0.885	S10
PPy/Rh_{350s}	61	51	0.063	This work

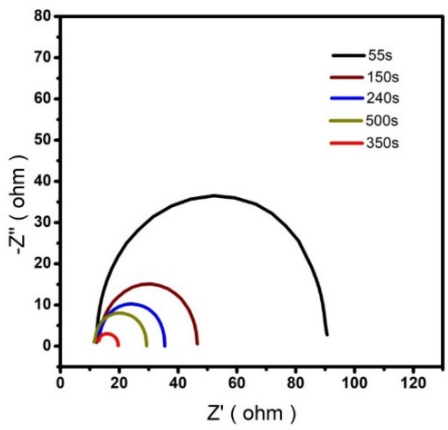

Fig. S11. The EIS of Rh/PPy with the different deposition time.

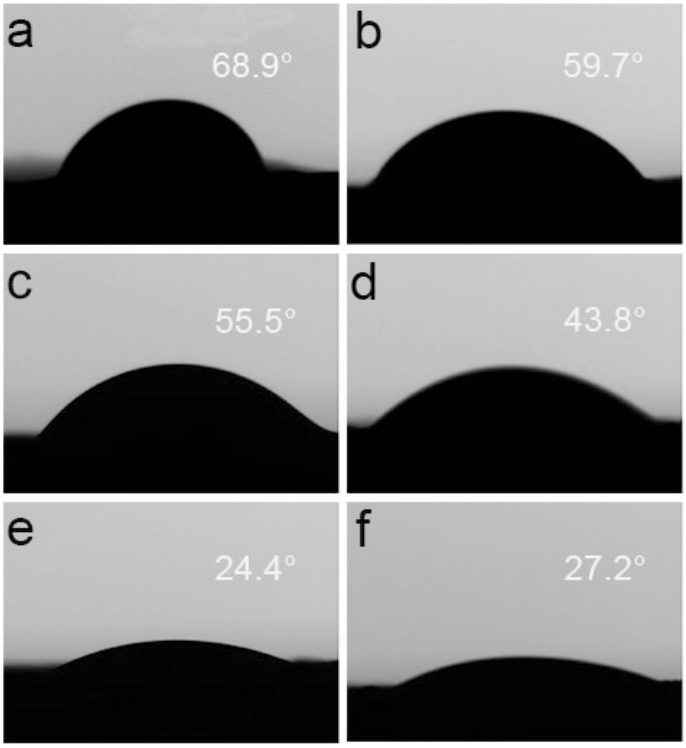

Fig. S12. Contact Angle test of hydrophilic acidity of a) PPy; b) Rh/PPy$_{55s}$; c) Rh/PPy$_{150s}$; d) Rh/PPy$_{240s}$; e) Rh/PPy$_{350s}$; f) Rh/PPy$_{500s}$.

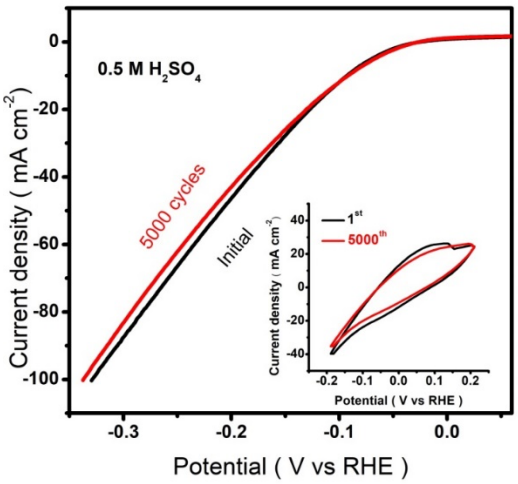

Fig. S13. The LSV curve of Rh/PPy$_{350s}$ before and after 5000 cycles, inset is CV curve of first cycle and 5000th cycles.

Supplementary References

1. K. Wang, B. L. Huang, F. Lin, F. Lv, M. C. Luo, P. Zhou, Q. Liu, W. Y. Zhang, C. Yang, Y. H. Tang, Y. Yang, W. Wang, H. Wang and S. J. Guo, *Adv. Energy Mater.*, 2018, **8**, 1801891.
2. F. L. Yang, Y. M. Zhao, Y. S. Du, Y. T. Chen, G. Z. Cheng, S. L. Chen and W. Luo, *Adv. Energy Mater.*, 2018, **8**, 1703489.
3. W. Shen, L. Ge, Y. Y. Sun, Fan. Liao, L. Xu, Q. Dang, Z. H. Kang and M. W. Shao, *ACS Appl. Mater. Interfaces*, 2018, **10**, 33153-3161.
4. B. B. Jiang, L. L. Yang, F. Liao, M. Q. Sheng, H. Z. Zhao, H. P. Lin and M. W. Shao, *Nano Research*, 2017, **10**, 1749-1755.
5. L. L. Zhu, H. P. Lin, Y. Y. Li, F. Liao, Y. Lifshitz1, M. Q. Sheng, S-T Lee and M. W. Shao, *Na*t. Commun., 2016, **7**, 12272.
6. T. Kim, J. Park, H. Jin, A. Oh, H. Baik, S. H. Joo and K. Lee, *Nanoscale*, 2018, **10**, 9845-9850.
7. M. Akbayrak and A. M. Önal, *J. Electrochem. Soc*, 2019, **166**, 897-903.
8. D. Yoon, B. Seo, J. Lee, K. S. Nam, B. Kim, S. Park, H. Baik, S. H. Joo and K. Lee, *Energy Environ. Sci.*, 2016, **9**, 850-856.
9. Y. F. Cheng, S. K. Lu, F. Liao, L. B. Liu, Y. Q. Li and M. W. Shao, *Adv. Funct. Mater.*, 2017, **27**, 1700359.
10. Q. Wang, B. Xu, C. L. Xu, Y. Wang, Y. Zhang, J. Wu and G. Y. Fan, *Appl. Surf. Sci.*, 2019, **495**, 143569.